12th World Congress on Structural and Multidisciplinary Optimization
5th - 9th, June 2017, Braunschweig, Germany

Metamodel-based global optimization of vehicle structures for crashworthiness supported by clustering methods

Kai Liu[1], Duane Detwiler[2], Andres Tovar[3]

[1] Purdue University, West Lafayette, Indiana, USA, liu915@purdue.edu
[2] Honda R&D Americas, Inc., Raymond, Ohio, USA, ddetwiler@oh.hra.com
[3] Indiana University - Purdue University Indianapolis, Indianapolis, USA, tovara@iupui.edu

1. Abstract

This work introduces a metamodel-based global optimization method for crashworthiness with the ability to synthesize continuum structures with an optimal distribution of material phases or gauges. The proposed optimization method makes use of fully nonlinear, dynamic crash simulations and consists of three main elements: (1) the generation of a conceptual design from the structures crash response, (2) the optimal clustering of the conceptual design to define the location of the material phases or gauges, (3) the metamodel-based global optimization, which aims to find the optimal settings for each cluster. The conceptual design can be generated from extracting finite element analysis information or by using structural optimization. The conceptual design is then clustered using clustering analysis to reduce the dimension of the design space. The global optimization problem aims to find the optimal material distribution on the reduced design space using metamodels. The metamodels are built using sampling and cross-validation, and sequentially updated using an expected improvement function until convergence. The proposed methodology is demonstrated using examples from multi-objective crashworthiness design examples.

2. Keywords: crashworthiness, metamodel, structural optimization, clustering

3. Introduction

Vehicle crashworthiness relies heavily on the energy absorbing capabilities of plastically deformable progressive crushing zones located at the front and rear end of the vehicle's body. In commercial vehicles, progressive crushing zones are comprised of thin-walled structures arranged in the form of hollow tubes, which are ultimately responsible for managing impact energy in the event of a collision. Thin-walled components are highly formable, structurally sound, and capable of sustaining axial collapse mode. This collapse mode, also known as progressive folding, is achievable by tubes of uniform thickness under axial load [1]. Geometric and material discontinuities as well as strain-rate effects and oblique impact promote a less desirable bending collapse mode. This low-energy collapse mode, also known to as Euler-type buckling, reduces the component crashworthiness and increases the risk of damage and intrusion in other zones of the vehicle [2]. In order to mitigate this undesirable Euler-type buckling, vehicle structural designers have incorporated design features, such as crush initiators in the form of cutouts, dents, and stiffeners [3, 4, 5], or integration of design optimization method [6, 7] and the use of topology optimization [8, 9, 10].

In this study, we introduced an systematic approach that is not only able to generate initial progressive folding conceptual design, but also capable of further optimize the structure using multi-objective structural optimization. The conceptual design is a continuous design variable distribution that can be generated from a finite element analysis field or from structural optimization. Clustering allows the dimension reduction of the structure from thousands of design variables to less than 20. With the reduced number of design variables, metamodel-based global optimization can be performed efficiently and effectively.

4. Conceptual Design

The first step in the proposed strategy is to generate a conceptual design (field variable). The conceptual design can be generated in two ways: (1) from the solution of a related structural optimization problem, and (2) from the distribution of a finite element field, e.g., strain field, stress field. Let us consider the case of generating a conceptual design from a related structural optimization. In this case, a material property is characterized by a parameter $x \in \mathbb{R}$, where $0 \leqslant x \leqslant 1$. Then, the conceptual design problem is to find the distribution of all possible parameterized materials $\mathbf{x} \in \mathbb{R}^n$ in a discretized structure with n discrete elements that minimize the objective function $f(\mathbf{x}) : \mathbb{R}^n \rightarrow \mathbb{R}$ subjected to a set of (equality and inequality) constraints. Thus, the constrained optimization problem is

This is the author's manuscript of the article published in final edited form as:
Liu, K., Detwiler, D., & Tovar, A. (2018). Metamodel-Based Global Optimization of Vehicle Structures for Crashworthiness Supported by Clustering Methods. In A. Schumacher, T. Vietor, S. Fiebig, K.-U. Bletzinger, & K. Maute (Eds.), Advances in Structural and Multidisciplinary Optimization (pp. 1545–1557). Springer International Publishing. https://doi.org/10.1007/978-3-319-67988-4_116

expressed as:

$$\begin{aligned} \text{find} \quad & \mathbf{x} \in \mathbb{R}^n \\ \text{minimize} \quad & f(\mathbf{x}, \mathbf{U}(\mathbf{x}), t)) \\ \text{subject to} \quad & \mathbf{h}(\mathbf{x}, \mathbf{U}(\mathbf{x}), t) = \mathbf{0} \\ & \mathbf{g}(\mathbf{x}, \mathbf{U}(\mathbf{x}), t) \leqslant \mathbf{0} \\ & 0 \leqslant x_e \leqslant 1, \quad e = 1, \ldots, n, \end{aligned} \tag{1}$$

satisfying finite element equilibrium equations. Several algorithms found in literature are appropriate to solve the structural optimization [11]. The result is an optimal distribution with up to n materials within the structure. For a moderate finite element model, n is in the order of 10^3 to 10^6. This value is too high to utilize metamodel-based optimization. The number of inputs to a metamodel is typically within twenty. To reduce the dimensionally of the design space from $\mathbb{R}^n$ to $\mathbb{R}^K$, we propose the use of clustering method, which is presented in the following section.

5. Clustering

Many clustering analysis and dimensionally reduction methods are available in the field of machine learning, including K-means clustering, Expectation Maximization clustering, and Principle Component Analysis. However, despites the widely used of the methods mentioned above for the clustering analysis, it is difficult to impose constraints during the clustering analysis. In this investigate, we propose the use of 1D optimization method to perform clustering analysis. Each cluster has three design parameters, i.e., lower bound, upper bound and cluster center. The lower bound and upper bound define an envelop where all the field variables within the envelop are considered to be one cluster. The cluster center is simply assigned as the mean value of the field variables in the cluster. Such values will be optimized during the metamodel-based optimization. Assuming the envelop defining each cluster does not overlap, the 1D optimization problem to find K clusters can be posted as:

$$\begin{aligned} \text{find} \quad & \theta \in \mathbb{R}^{K-1} \\ \text{minimize} \quad & f(\mathbf{x}(\theta)) \\ \text{subject to} \quad & \mathbf{h}(\mathbf{x}(\theta)) = \mathbf{0} \\ & \mathbf{g}(\mathbf{x}(\theta)) \leqslant \mathbf{0} \\ & x_{\min} \leqslant \theta_1 \leqslant \cdots \leqslant \theta_k \ldots \leqslant \theta_{K-1} \leqslant x_{\max}, \end{aligned} \tag{2}$$

where the objective function f and constraints $\mathbf{h}, \mathbf{g}$ could be same as the conceptual design. In such cases, more finite element analyses are required to generate the clustered design. In our example, we choose the objective function such that the average value of the field variable in the clustered design is the same as the conceptual design without any further finite element analysis. Once the optimal parameters θ are found, the lower bound and upper bound for each cluster can be assigned as $[\theta_{k-1}, \theta_k)$ where $k = 1, \ldots, K$, $\theta_0 = x_{\min}, \theta_K = x_{\max}$. The cluster for each element can be then assigned based on the envelop defined by each cluster. Let S_k be the set of elements for the k-th cluster. The value of $x_e \in S_k$ is then replaced by the cluster center μ_k. The resulting K-dimensional clustered design is suitable for building metamodels and performing optimization.

6. Generation of initial metamodel

Dynamic models involving geometric, material, and contact nonlinearities are commonly found in crash simulations [10]. For such models, the computational cost of a function evaluation is considerably high and it is impractical to use traditional gradient-based optimization methods due to the lack of reliable sensitivity coefficients. As an alternative, metamodels can be derived by sampling the dynamic, nonlinear finite element model. The resulting metamodels are numerically inexpensive and allow to find near-optimal solutions through the use of global multi-objective algorithms [12]. The key aspect to using metamodels for global optimization lies in balancing between exploration (size) and exploitation (accuracy). It is desirable to generate an accurate metamodel that explores a large portion of the design space with a few sampling points. The Efficient Global Optimization algorithm is used to strick the balance between between exploration and exploitation. However, metamodels need to be built and validated prior to the EGO algorithm. Some key concepts including sampling and cross validation are briefly discussed in this section and the metamodel-based global optimization algorithm is given in Sec 7.

6.1 Sampling

Computer design of experiments is the selection procedure for finding the points in the design space that must be simulated. Many strategies can be used to sample the design points including factorial designs, D-optimal designs,

and Latin hypercube sampling (LHS) [13]. LHS is used in this work to generate the initial metamodel. This provides designs that are independent of the mathematical model of the approximation and allow the estimation of the main effects of all factors in the design in an unbiased manner. Another advantage of LHS is the number of points to be evaluated can be directly defined. For K clusters (design variables) and P design points, the LHS provides a $P \times K$ matrix $\mathbf{S}$ that randomly samples the entire design space broken down into P equal-probability regions.

6.2 Cross-validation

With the initial samples, Kriging metamodel is built for each objectives. Despite the number and optimal distribution of the sampled designs, the resulting metamodel may not be sufficiently accurate to provide meaningful predictions. To estimate the accuracy of the metamodel and avoid any unnecessary expensive finite element analysis, this work uses the leave-one-out cross-validation. In this cross-validation approach, one design is left out from the P sampled designs; then, the metamodel is re-generated using the remaining $P-1$ designs (Fig. 1). If $\mathbf{S}^{(p)}$ is the pth sampled design that has been left out, $f(\mathbf{S}^{(p)})$ the function value, and $\hat{f}_{-p}(\mathbf{S}^{(p)})$ be the cross-validated prediction of $f(\mathbf{S}^{(p)})$, then one can plot $\hat{f}_{-p}(\mathbf{S}^{(p)})$ against $f(\mathbf{S}^{(p)})$. If the metamodel fits perfectly, these points should lie on the 45° line [14]. If this diagnostic plot looks satisfactory, e.g., high coefficient of determination R^2, then the metamodel is also considered satisfactory; otherwise, the metamodel is refit with a log or inverse transformation to the dependent variable. If one of these transformations gives satisfactory diagnostic plot, then this transformation function is used in the rest of the analysis.

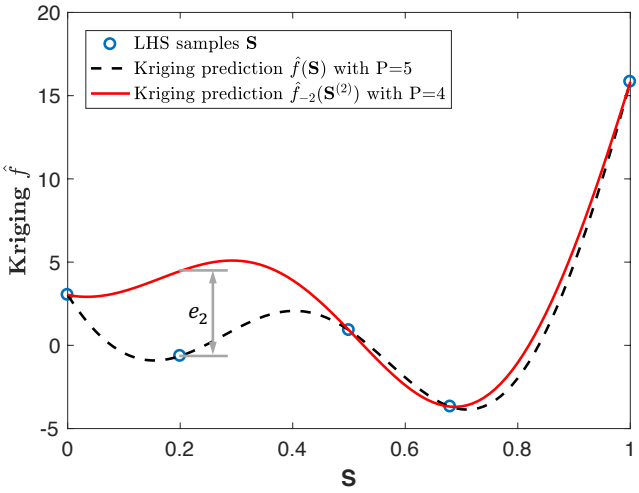

Figure 1: Leave-one-out cross-validation at the second sampled point exemplified by fitting a function with a Kriging model.

7. Metamodel-based Global Optimization

Once the initial metamodels are built, the global optimization problem can be solved. The global optimization problem is to find the material parameters that minimize the objective function vector $\mathbf{f}(\mu) : \mathbb{R}^K \rightarrow \mathbb{R}^{n_f}$, where n_f is the number of objective functions. The input to the metamodels $\hat{\mathbf{f}}$ is the vector cluster center μ for each cluster. The output is the predicted values of the finite element models $\mathbf{f}$. The optimal design can be found using the Efficient Global Optimization (EGO) algorithm [14, 15]. During the search for the global optimum, the EGO algorithm iteratively improves the metamodels by sampling at the point where the expected improvement function is maximized. The expected improvement for a two objectives optimization problem is defined as [15]:

$$\mathrm{E}[I(\mathbf{S}^{*(p)})] = \mathrm{P}[I(\mathbf{S}^{*(p)})]\ \min\{d_1, \ldots, d_m\}, \tag{3}$$

where m is number of points on the Pareto front. $\mathrm{P}[I(\mathbf{S}^{*(p)})]$ is the probability of improving both functions f_1 and f_2 at the Pareto design $\mathbf{S}^{*(p)}$. The probability of improvement is defined as:

$$\mathrm{P}[I(\mathbf{S}^{*(p)})] = \Phi(u_1^i) + \sum_{i=1}^{m-1} \left[\Phi(u_1^{i+1}) - \Phi(u_1^i)\right] \Phi(u_2^{i+1}) + [1 - \Phi(u_1^m)]\,\Phi(u_2^m), \tag{4}$$

where $u_j^i = u_j^i(\mathbf{S}^{*(p)}) = \left(f_j^{*(i)} - \hat{f}_j(\mathbf{S}^{*(p)})\right)/\sigma_j(\mathbf{S}^{*(p)})$. $\left(f_1^{*(i)}, f_2^{*(i)}\right)$ is a Pareto point.

In Eq. (3), d_i for $i = 1,\ldots,m$ is the distance between the vectors $(\bar{F}_1,\bar{F}_2)$ and $\left(f_1^{*(i)}, f_2^{*(i)}\right)$, where $(\bar{F}_1,\bar{F}_2)$ is the centroid of the probability integral used to calculate $\mathrm{E}[I(\mathbf{S}^{*(p)})]$:

$$\bar{F}_1(\mathbf{S}^{*(p)}) = \frac{1}{\mathrm{P}[I(\mathbf{S}^{*(p)})]}\left[z_1^1 + \sum_{i=1}^{m-1}\left(z_1^{i+1} - z_1^i\right)\Phi(u_2^{i+1}) + z_1^m\Phi(u_2^m)\right] \tag{5}$$

where $z_j^i = z_j^i(\mathbf{S}^{*(p)}) = \hat{f}_j(\mathbf{S}^{*(p)})\Phi(u_j^i) - \sigma_j(\mathbf{S}^{*(p)})\phi(u_j^i)$. $\bar{F}_2(\mathbf{S}^{*(p)})$ is defined similarly. Details on the derivation of the multi-objective expected improvement formula can be found in [15].

8. Numerical Examples

8.1 Ball plate impact

This example considers the thickness (topometry) optimization of a base plate impacted by a rigid ball undergoing large displacement (Fig. 2). The goal is to minimize both the impact penetration and the mass of the plate. The dimension of the plate is 300 mm $\times$ 300 mm. The initial thickness of the plate is 5 mm. The plate is constrained along its four edges. The plate's finite element model is discretized into 30×30 identical finite elements. The rigid ball impacts the plate in a perpendicular direction at a speed of 10 m/s. The base material properties are listed in Table 1.

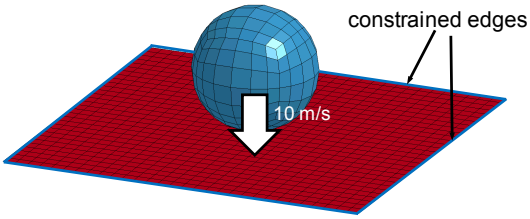

Figure 2: Initial design domain for minimum impact penetration

Table 1: Base material properties for the plate

Property	Value	
Density	7830	kg/m^3
Elastic Modulus	207	GPa
Poisson's Ratio	0.3	
Yield stress	200	MPa
Tangent modulus	2.0	GPa

Step 1: Conceptual design The conceptual design is generated using the von Mises strain at the maximum penetration. The simulation is performed using explicit nonlinear finite element analysis in the commercial code LS-DYNA (LSTC, California). The conceptual design is shown in Fig. 3. The contour indicates the value of the von Mises strain for each element–the higher the darker. The conceptual design is shown in 'o' in Fig. 5.

Figure 3: Conceptual design based on the von Mises strain distribution with maximum penetration $f_1 = 12.1$ mm and mass fraction $f_2 = 0.50$.

Figure 4: Clustered conceptual design with maximum penetration $f_1 = 9.76$ mm and mass fraction $f_2 = 0.50$.

Step 2: Clustered design Using the normalized von Mises strain as the field variable, the 1-D optimization problem with four clusters is solved. The solution to the optimization problem is a 3×1 vector $\boldsymbol{\theta} = [0.32, 0.59, 0.68]^T$. Hence, the lower bound lb, upper bound ub and mass fraction m_f for each cluster can be derived correspondingly as summarized in Table 2. The clustered design is shown in Fig. 4 and '$\diamond$' in Fig. 5.

Table 2: Optimal material parameters of the clustered design.

k	Color	lb_k	ub_k	m_{fk}
1	Blue (■)	0.68	1.00	0.17
2	Red (■)	0.58	0.68	0.29
3	Black (■)	0.32	0.58	0.29
4	Green (■)	0.00	0.32	0.25

Step 3: Metamodel-based global optimization The objectives are to minimize the maximum penetration during an impact and minimize plate mass. This problem can be stated as follows:

$$\begin{aligned} \text{find} \quad & \mu \in \mathbb{R}^K (K=4) \\ \text{minimize} \quad & f_1(\mathbf{x}(\mu)) : \text{ maximum penetration} \\ \text{minimize} \quad & f_2(\mathbf{x}(\mu)) : \text{mass fraction} \\ \text{subject to} \quad & 1 \leqslant \mu_k \leqslant 10, \quad k = 1,2,3,4. \end{aligned} \tag{6}$$

Kriging metamodels are built for both objective functions. Since both two objectives value can be achieve from one single function evaluation, the initial two metamodels are built with the same 40 LHS samples. EGO algorithm with multi-objective expected improvement is used for global search. The algorithm is stopped at 100 iterations, and the Pareto front is derived during the EGO process (Fig. 5). As expected, both the initial design and clustered design are dominated by several designs in the Pareto front (Fig. 5). The computational cost of this example is summarized in Table 3.

Notably, the conceptual design, which contains a large number of design variables, has roughly the same mass than the one of the clustered design but allows more penetration under impact. In this case, the clustered design may be a better alternative than the conceptual one. The use of metamodel-based multiobjective optimization allows to generating a Pareto front. This front includes, among other non-dominated designs, one that has same mass as the clustered design that results in 18% less penetration under impact. This shows the effectiveness of the proposed design methodology.

Figure 5: Pareto front of the design optimization problem. An design alternative shows maximum impact penetration $f_1 = 8.0$ mm and mass fraction $f_2 = 0.50$.

Table 3: 3SDO computational cost

step	# iter.	# feval
Conceptual	0	1
Clustering	20	0
Sampling	40	40
Optimization	100	100

8.2 Thin-walled S-rail crashworthiness design

Thin-walled S-rail structures are the central components of vehicles progressive crushing zones and absorb the highest amount of the kinetic energy during a frontal or rear collision. The design variable in this example is the element shell thickness of the structure. The design variables are the element shell thickness of the structure. The S-rail is impacted by a rigid wall with 5m/s prescribed displacement. Piecewise linear plastic material is used in this example. The objective is to maximize the crashworthiness of the structure measured by specific energy absorption (energy absorption per unit mass) and peak crushing force.

Step 1: Conceptual design The conceptual design aims to trigger the progressive collapse of the S-rail structure during the impact using the principle of the compliant mechanism. The design of a compliant mechanism using topometry optimization finds the thickness distribution that maximizes the displacement at the output port [16] or the mutual potential energy [17] subjected to an equality mass constraint. For a thin-walled S-rail structure as shown in Fig. 6, the input ports are prescribed at the contact nodes with a rigid wall. The output ports correspond to the desired buckling trigger locations. Such locations may be prescribed according to the designer's criterion. However, they are naturally assigned by the wavelength λ of the progressive buckling corresponding to an ideal axial crushing condition. The optimization problem can be stated as below:

Figure 6: Locations of input and output ports for a thin-walled S-Tube following the wavelength λ corresponding to the progressive buckling after an ideal axial crushing condition.

$$\begin{aligned} \text{find} \quad & \mathbf{x} \in \mathbb{R}^n \\ \text{minimize} \quad & f(\mathbf{x}, \mathbf{U}(\mathbf{x})) = -u_{\text{out}}(\mathbf{x}, \mathbf{U}(\mathbf{x})) = -\mathbf{L}^{\mathrm{T}}\mathbf{U}(\mathbf{x}) \\ \text{subject to} \quad & h(\mathbf{x}) = \frac{1}{n}\sum_{e=1}^{n} x_e - m_f = 0 \\ & \underline{\mathbf{x}} \leqslant \mathbf{x} \leqslant \bar{\mathbf{x}}. \end{aligned} \tag{7}$$

where $\mathbf{L}$ is a unit length vector with zeros at all degrees of freedom except at the output point where it is one. The term $\mathbf{L}^{\mathrm{T}}\mathbf{U}$ is referred to as Mutual Potential Energy (MPE). $\underline{\mathbf{x}} = 6 \times 10^{-4} m$, $\bar{\mathbf{x}} = 6 \times 10^{-3} m$, and $m_f = 0.50$. In this example, Hybrid Cellular Automata (HCA) [18] is used as optimum search algorithm for this non-linear problem. The initial design is thickness uniformly distributed structure, and crash simulation of shows bulking at the beginning of crash event (Fig. 7). The conceptual design solution and its crash simulation are shown in Fig. 8 with progress folding pattern observed at the near impact end.

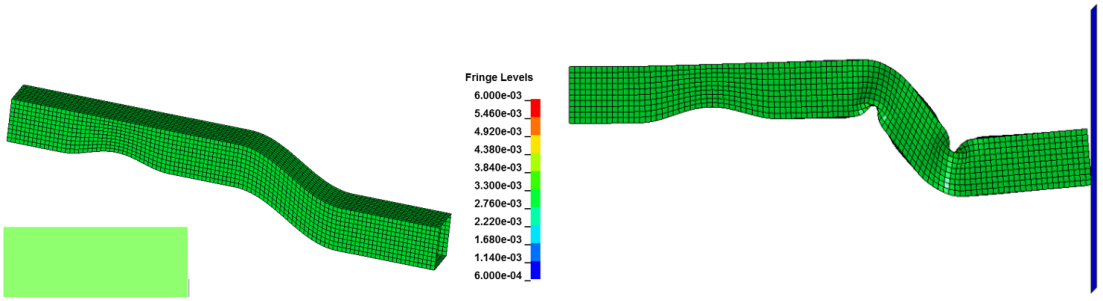

Figure 7: Initial design and its crash simulation

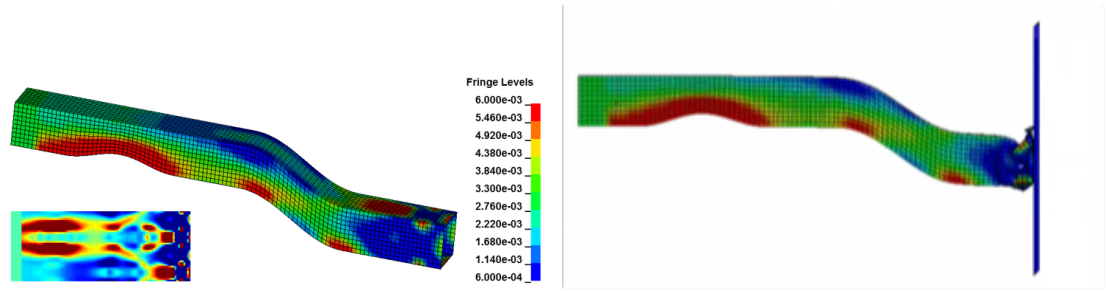

Figure 8: Conceptual design and its crash simulation.

The crashworthiness of the structure is measured by Specific Energy Absorption (SEA) U_a, Peak Crushing Force (PCF) $P_{\max}$, which are defined as:

$$U_a(\mathbf{x}) = \frac{\int_\delta P(\mathbf{x},\delta) d\delta}{m(\mathbf{x})}, \tag{8}$$

$$P_{\max}(\mathbf{x}) = \max_\delta P(\mathbf{x},\delta), \tag{9}$$

where $P(\mathbf{x},\delta)$ is the reaction force of the thin-walled component at a crushed distance δ. The simulation of the thin-walled crushing requires the use of non-linear finite element analysis.

The crashworthiness of the initial and conceptual structure are summarized in Table 5 and are plotted in Fig. 10 as '$\circ$' and '$\square$', respectively. In comparison to the initial design, the conceptual design shows 48.97% specific energy absorption increments yet 34.12% increases in the peak crushing force.

Step 2: Clustered design In this example, the conceptual design is derived from density-based structural optimization. The element density is used as the field variable to cluster the design. The 1-D optimization problem as shown in Eq. (2) is then solved. Four clusters is considered in this example. The optimization problem is solved in 30 iterations. The solution vector $\theta = [0.39, 0.46, 0.66]^T$. The clusters generated in this step are summarized in Table 4. Figure 9 demonstrates the clustered design. The last row of Table 5 gives the crashworthiness measurements of the clustered design and it is also plotted in Fig. 10 as '$\diamond$'.

Table 4: Optimal material parameters of the clustered design.

k	Color	lb_k	ub_k	m_{fk}
1	Red	0.66	1.00	0.24
2	Black	0.46	0.66	0.25
3	Blue	0.39	0.46	0.19
4	Green	0.00	0.39	0.32

Figure 9: Clustered conceptual design

Table 5: Comparison of the crashworthiness

	U_a (kJ/kg)	$P_{\max}$ (kN)
Initial	3.39	267.39
Conceptual	5.05	358.63
Clustered	5.02	331.51

Step 3: Metamodel-based global optimization For this thin-walled S-rail crashworhtiness design problem, the design objectives are to minimize the peak crushing force and maximize the specific energy absorption. This problem can be stated as follows:

$$\begin{aligned} \text{find} \quad & \mu \in \mathbb{R}^K (K=4) \\ \text{maximize} \quad & f_1(\mathbf{x}(\mu)) : U_a(\mathbf{x}(\mu)) \\ \text{minimize} \quad & f_2(\mathbf{x}(\mu)) : P_{\max}(\mathbf{x}(\mu)) \\ \text{subject to} \quad & 6\times 10^{-4} \leqslant \mu_k \leqslant 6\times 10^{-3}, \quad k=1,2,3,4. \end{aligned} \tag{10}$$

Kriging metamodels are built for both objective function with 40 initial LHS samples. The EGO algorithm with multi-objective expected improvement stops after 100 iterations. Figure 10 shows the Pareto front that is derived from the EGO algorithm. The Pareto front clearly dominates the initial design. The conceptual design is close to the Pareto front, however, the conceptual design has more than 4000 design variables while the designs on the Pareto front has only 4 design variables. The clustered design on the other hand is part of the Pareto front that generated using the metamodel-based global optimization. Table 6 summarizes the computational cost.

Table 6: 3SDO computational cost

Figure 10: Pareto front of the design optimization problem.

step	# iter.	# feval
Conceptual	1	2
Clustering	30	0
Sampling	40	40
Optimization	100	100

9. Summary and Discussion

This work presents a design approach to solve nonlinear structural optimization problems. The proposed algorithm consists of three steps: conceptual design generation, clustering, and metamodel-based global optimization. The conceptual design is a continuous design variable distribution that can be generated from a finite element analysis field (Sec. 8.1) or from structural optimization (Sec. 8.2). Clustering analysis allows the dimension reduction of the structure from thousands of design variables to less than 20. With the reduced number of design variables, metamodel-based global optimization can be performed efficiently and effectively. The proposed method is demonstrated through two multi-objective design optimization examples: ball plate impact and thin-walled S-rail crashworthiness design. Both examples are solved using dynamic nonlinear finite element analysis.

Aspects of the proposed structural optimization approach can be modified to solve specific problems. For example, instead of using topology optimization as illustrated in the paper, topograghy optimization can be applied. For clustering, K-means can be replaced with Principle Component Analysis or other machine learning method. Supervisions can be also introduced to design characterization. While designers have the freedom to choose the number of materials, the number of materials is limited by manufacturing capabilities and metamodel techniques.

One important issue that is not explored in this investigation is how to choose the optimal number of clusters (or materials). The optimal choice the number of clusters K is often ambiguous. Some methods to choose K including the rule of thumb, the elbow method, information criterion approach, and the Silhouette method [12]. Another ongoing investigation is how to reduce the structural complexity of the result generated by the proposed approach; generally, this can be controlled in the initial design generation stage and/or using clustering algorithm that has more control on how the variables are grouped together.

10. Acknowledgment

Honda R&D Americas supported this research effort. Any opinions, findings, conclusions, and recommendations expressed in this investigation are those of the writers and do not necessarily reflect the views of the sponsors.

11. References

[1] Z. Kazanc and K.-J. Bathe, "Crushing and crashing of tubes with implicit time integration," *International Journal of Impact Engineering*, vol. 42, pp. 80 – 88, 2012.

[2] N. Jones and T. Wierzbicki, "Structural crashworthiness and failure," 1993.

[3] F. Samer, F. Tarlochan, P. Khalili, and H. Samaka, "Enhancement of energy absortion of thin walled hexagonal tube by using trigger mechanisms," *International Journal of Research in Engineering and Technology*, vol. 2, no. 8, pp. 109–116, 2013.

[4] M. Shakeri, R. Mirzaeifar, and S. Salehghaffari, "New insights into the collapsing of cylindrical thin-walled tubes under axial impact load," in *the Institution of Mechanical Engineers, Part C: Journal of Mechanical Engineering Science*, vol. 221, no. 8, 2007.

[5] S. Salehghaffari, M. Tajdari, M. Panahi, and F. Mokhtarnezhad, "Attempts to improve energy absorption characteristics of circular metal tubes subjected to axial loading," *Attempts to improve energy absorption characteristics of circular metal tubes subjected to axial loading*, vol. 48, no. 6, pp. 379–390, 2010.

[6] G. Sun, G. Li, S. Hou, S. Zhou, W. Li, and Q. Li, "Crashworthiness design for functionally graded foam-filled thin-walled structures," *Materials Science and Engineering A-structural Materials Properties Microstructure and Processing*, vol. 527, pp. 1911–1919, 2010.

[7] H. Yin, G. Wen, S. Hou, and Q. Qing, "Multiobjective crashworthiness optimization of functionally lateral graded foam-filled tubes," *Materials & Design*, vol. 44, pp. 414 – 428, 2013.

[8] J. K. Paik, B. J. Kim, D. K. Park, and B. S. Jang, "On quasi-static crushing of thin-walled steel structures in cold temperature: Experimental and numerical studies," *International Journal of Impact Engineering*, vol. 38, no. 1, pp. 13 – 28, 2011.

[9] R. R. Mayer, N. Kikuchi, and R. A. Scott, "Application of topological optimization techniques to structural crashworthiness," *International Journal for Numerical Methods in Engineering*, vol. 39, no. 8, pp. 1383–1403, 1996.

[10] P. Bandi, J. P. Schmiedeler, and A. Tovar, "Design of crashworthy structures with controlled energy absorption in the hybrid cellular automaton framework," *Journal of Mechanical Design*, vol. 135, no. 091002, pp. MD–12–1267, 2013.

[11] P. W. Christensen and A. Klarbring, *An introduction to structural optimization.* Springer, 2009.

[12] K. Liu, A. Tovar, E. Nutwell, and D. Detwiler, "Thin-walled compliant mechanism component design assisted by machine learning and multiple surrogates," in *SAE World Congress*, 2015.

[13] R. Myers and D. Montgomery, *Response Surface Methodology. Process and Product Optimization using Designed Experiments.* Wiley, 1995.

[14] D. R. Jones, M. Schonlau, and W. J. Welch, "Efficient global optimization of expensive black-box functions," *Journal of Global Optimization*, vol. 13, pp. 455–492, 1998.

[15] A. I. J. Forrester, A. Sóbester, and A. J. Keane, *Engineering Design via Surrogate Modelling - A Practical Guide*. Wiley, 2008.

[16] O. Sigmund and S. Torquato, "Design of materials with extreme thermal expansion using a three-phase topology optimization method," *Journal of the Mechanics and Physics of Solids*, vol. 45, no. 6, pp. 1037 – 1067, 1997. [Online]. Available: http://www.sciencedirect.com/science/article/pii/S0022509696001147

[17] A. Saxena and G. Ananthasuresh, "On an optimal property of compliant topologies," *Structural and Multidisciplinary Optimization*, vol. 19, no. 1, pp. 36–49, 2000.

[18] A. Tovar, N. M. Patel, G. L. Niebur, M. Sen, and J. E. Renaud, "Topology optimization using a hybrid cellular automation method with local control rules," *Journal of Mechanical Design, Transactions of the ASME*, vol. 128, no. 6, pp. 1205–1216, 2006.